Adaptive Reactionless Motion Control for Free-Floating Space Manipulators

Shuanfeng Xu, Hanlei Wang, Duzhou Zhang, and Baohua Yang

arXiv:1402.5586v1 [cs.SY] 23 Feb 2014

***Abstract*—This paper investigates the adaptive version of reaction null-space (RNS) based control for free-floating space manipulators with uncertain kinematics and dynamics in the presence of nonzero initial angular and linear momenta. The great challenge in deriving the adaptive RNS-based control scheme is that it is difficult to obtain a linear expression which is the basis of the adaptive control. The main contribution of this paper is that we skillfully obtain such a linear expression, based on which, an adaptive version of the RNS-based controller is developed at velocity level, taking into account both the kinematic and dynamic uncertainties. It is shown that the proposed control achieves both the base attitude regulation and continuous path tracking of the end-effector. The simulation results are presented to show the effectiveness of the proposed controller.**

I. Introduction

ON-ORBIT servicing (OOS) has become one of the current hot areas of research for space agencies. For some human manipulation tasks in hazardous space environment, e.g., transferring payloads from one place to another, executing repairing, maintenance and construction of spacecraft or space station, and capturing tumbling satellite, the hazard and cost-intensity of human space-transportation system impedes such application to most spacecraft systems. Accordingly, robotics are now assisting the human as the human-extended arm in space [1]. Robotic manipulators in space environments are usually mounted on a movable spacecraft, and such a robotic-spacecraft system is the well-known space manipulators. OOS demonstration missions such as the Japanese Engineering Test Satellite VII (ETS-VII) [2], Rokviss [3], and Orbital Express [4] are successful examples which have shown how to effectively exploit the exploration and manipulation capabilities of robots in space using different approaches. However, such tasks executed by space robots are inherently subject to large kinematic and dynamic uncertainties. Under large parameter uncertainties or variations, model based controllers tend to lower the tracking accuracy or even drive the system unstable [5]. Thus, it is important to develop robot controllers that can deal with uncertainties in both kinematics and dynamics. Adaptive control, as a standard control methodology, is a qualified approach to solve this problem. A prediction error based adaptive Jacobian controller was proposed to attack task-space trajectory tracking of free-floating space robots with uncertain kinematics and dynamics [6].

Among the control modes of space manipulators, free-floating space manipulators (FFSM) have their potential advantages [7]. First, the unrenewable and thus precious fuel can be saved since both the position and the attitude of the spacecraft are not actively controlled in this case, so the life of the system will be extended. Second, hazardous and even fatal collisions that may be induced by the action of the attitude control system can be avoided in the free-floating mode of operation when the servicing spacecraft is very close to or in contact with the target spacecraft [3].

It is known that in a free-floating space robotic system, due to the lack of a fixed base, the spacecraft will move in response to the dynamic forces caused by the manipulator's motion, and the motion of the whole system is governed by the principle of momentum conservation. However, from a practical point of view, it is important to keep the base attitude unchanged as the spacecraft has to always point its antenna toward the Earth, whereas disturbing the base translation does not pose any significant side effect [8]. Hence, joint motion algorithms for space manipulators without reaction to the base are highly preferred. On the other hand, the manipulator end-effector is usually required to track some trajectory in Cartesian space when executing OOS. Thus, it is meaningful to realize coordinated spacecraft/manipulator motion control.

Many researchers have studied coordination control of a manipulator and its free-floating base. Vafa and Dubowsky proposed cyclic motion of the manipulator joints to change the base orientation [9]. Nakamura and Mukherjee utilized Lyapunov function to achieve the regulation of both the base attitude and the manipulator joint angles simultaneously [10]. Inspired by the fact that a falling cat changes its orientation in midair without violating angular momentum constraints, Fernandes et al. investigated motion planning for a system of coupled rigid bodies, which can be used for space robotic applications, such as attitude control of the base spacecraft using internal motion [11]. Dubowsky and Torres proposed EDM (Enhanced Disturbance Map) to plan the trajectory of space manipulators with minimum disturbance on the base attitude [12]. Yamada used the variational method to find a closed trajectory of manipulator joints that generates an arbitrary change of the base attitude [13]. Suzuki and Nakamura proposed "spiral motion" of the end-effector to achieve arbitrary change of the base attitude and the manipulator joint angles, which is unfortunately an approximate method [14]. Tortopidis and Papadopoulos presented a method to accom-

S. Xu, H. Wang and D. Zhang are with Science and Technology on Space Intelligent Control Laboratory, Beijing Institute of Control Engineering, Beijing, 100190, China (e-mail: strivesfxu@gmail.com; hlwang.bice@gmail.com; zhangduzhou@gmail.com).

B. Yang is with China Academy of Space Technology, Beijing, 100094, China (e-mail: bhyang.cast@gmail.com).

This work is supported by the National Natural Science Foundation of China under Grant 61004058 and the National Key Basic Research Program (973) of China under Grant 2013CB733100.

plish point-to-point planning for FFSM [15], in which high order polynomials are used to specify the desired path directly in joint-space. Nenchev et al. analyzed a redundant free-floating space/manipulator system based on the momentum conservation equations [16], where the concept of Reaction Null-Space originated. Two tasks can be realized: 1) end-effector continuous path tracking with simultaneous attitude maintenance; 2) changing the attitude of the base satellite while keeping fixed position/orientation of the end-effector with respect to either the inertial coordinate frame or a relative coordinate frame. To sum up, only the RNS based method can achieve the base attitude regulation with simultaneous manipulator end-effector continuous path tracking.

Reaction Null-Space has its root in the work of [16]. The RNS-based control law was originally proposed to cope with the dynamic interaction problem of flexible structure mounted manipulator systems [17]. A kinematic control scheme based on reaction null-space can achieve reactionless manipulation, or Zero Reaction Maneuver, where a combined inertia and Jacobian matrix is introduced [18]. The RNS-based reactionless manipulation was carried out and verified in the ETS-VII project [19]. Later, the implementation of the RNS-based controller for end-effector path tracking with reactionless motion and vibration suppression was proposed in [20]. A reactionless trajectory generation strategy was developed without affecting the attitude of the base for the capture of a target by a 2-DOF manipulator [21]. However, it should be noted that the methods proposed above all require the exact knowledge of both the kinematics and dynamics of the manipulator.

In the presence of parameter uncertainties or variations, only a few controllers have been developed attempting to resolve this problem. The great challenge is that it is difficult to find an appropriate linear expression which is the basis of designing parameter adaptation law. Taking dynamic uncertainties into consideration, adaptive reactionless motion algorithm for space manipulator was proposed in [22]. However, there is a problem in deriving the linear expression which acts as the basis of the adaptive reactionless control algorithm (ARLC), i.e., the designed velocity in this expression depends on the actual values of the dynamic parameters so that it is not measurable and thus unknown in the control, which leads to a result that the expression cannot be used to derive the ARLC. In addition, only the angular velocity of the base spacecraft is considered. However, the attitude of the base spacecraft will be affected during the adaptive control, which is undesirable in practice.

In this study, we skillfully obtain a linear expression which can be used to estimate the unknown parameters. Based on the linear expression, we propose an adaptive reactionless motion control algorithm that can deal with both the dynamic and kinematic uncertainties. These uncertainties could arise from the lack of accurate knowledge of the manipulator parameters or the unknown target that is captured by the manipulator, so our algorithm can also handle the capture problem. In contrast to the work of [22], the proposed algorithm can regulate the attitude of the base spacecraft during the adaptive control. Step by step, the joint motion algorithm is designed at velocity level to achieve 1) the base attitude regulation with simultaneous optimization of a rather general performance index, and 2) both the base attitude regulation and continuous path tracking of the end-effector. The main contribution of our work lies in that it gives the adaptive version of the RNS-based controller. Furthermore, taking the effects of nonzero initial linear and angular momenta into consideration, the algorithm proposed in this paper can still achieve both the base attitude regulation and continuous path tracking of the end-effector. A preliminary version of this paper appears in [23], which only considers the case where there are zero initial momenta, and, in this paper, we extend the previous algorithm to the case where there are nonzero initial momenta.

The paper is organized as follows: in Section II, the dynamics and kinematics which characterize a free-floating space robot, and the derivation of RNS are explained. Then, the formulation of adaptive reactionless motion controller is developed in Section III. To demonstrate the effectiveness of the proposed method, simulation results are shown in Section IV. Finally, the conclusions and future work are stated in Section V.

II. PRELIMINARIES

A. Dynamics of FFSMs

The equations of motion of a free-floating space robot explicitly including the rotational motion of the spacecraft are described by [24], [25]

$$\begin{bmatrix} \mathbf{H}_b & \mathbf{H}_{bm} \\ \mathbf{H}_{bm}^{\mathrm{T}} & \mathbf{H}_m \end{bmatrix} \begin{bmatrix} \dot{\boldsymbol{\omega}}_b \\ \ddot{\boldsymbol{\phi}} \end{bmatrix} + \begin{bmatrix} \mathbf{c}_b \\ \mathbf{c}_m \end{bmatrix} = \begin{bmatrix} \mathbf{0} \\ \boldsymbol{\tau} \end{bmatrix} \tag{1}$$

where $\boldsymbol{\omega}_b \in \mathbb{R}^3$ denotes the angular velocity of the base satellite with respect to the inertial frame expressed in the spacecraft frame, $\dot{\boldsymbol{\phi}} \in \mathbb{R}^n$ denotes the motion rate of the manipulator joints, $\boldsymbol{\phi} = \left[\phi_1, \ldots, \phi_n\right]^{\mathrm{T}}$ is the joint angle vector, $\mathbf{H}_b \in \mathbb{R}^{3\times 3}$ is the inertia matrix of the base, $\mathbf{H}_m \in \mathbb{R}^{n\times n}$ is the inertia matrix of the manipulator, $\mathbf{H}_{bm} \in \mathbb{R}^{3\times n}$ is the coupled inertia matrix of the spacecraft and the manipulator, $\mathbf{c}_b \in \mathbb{R}^3$ is the velocity-dependent nonlinear term of the base, $\mathbf{c}_m \in \mathbb{R}^n$ is the velocity-dependent nonlinear term of the manipulator, and $\boldsymbol{\tau} \in \mathbb{R}^n$ is the manipulator joint torque.

In the case of nonzero initial angular momentum, the integral of the upper set of (1) with respect to time gives [19]

$$\mathbf{R}_t(t)(\mathbf{H}_b\boldsymbol{\omega}_b + \mathbf{H}_{bm}\dot{\boldsymbol{\phi}}) \doteq \bar{\mathbf{H}}_b\boldsymbol{\omega}_b + \bar{\mathbf{H}}_{bm}\dot{\boldsymbol{\phi}} = \mathbf{L}_0 \tag{2}$$

where $\bar{\mathbf{H}}_b = \mathbf{R}_t(t)\mathbf{H}_b$, $\bar{\mathbf{H}}_{bm} = \mathbf{R}_t(t)\mathbf{H}_{bm}$, $\mathbf{L}_0$ is the initial angular momentum of the space manipulator system, $\mathbf{R}_t(t) \in SO(3)$ is the spacecraft orientation matrix with respect to the inertial frame, and $\bar{\mathbf{H}}_{bm}\dot{\boldsymbol{\phi}}$ represents the angular momentum generated by the manipulator motion. The momentum conservation equation (2) is simpler than the equation of motion at acceleration level, yet, reflects almost all aspects of the system dynamics [26].

Equation (2) depends linearly on a set of dynamic parameters $\mathbf{a}_d = \left[a_{d1}, a_{d2}, \ldots, a_{dp}\right]^{\mathrm{T}}$ and the initial angular

momentum $\mathbf{L}_0$ [27]

$$\begin{aligned}&\bar{\mathbf{H}}_b\boldsymbol{\omega}_b+\bar{\mathbf{H}}_{bm}\dot{\boldsymbol{\phi}}-\mathbf{L}_0\\&=\begin{bmatrix}\mathbf{Y}_d(\boldsymbol{\epsilon}_b,\boldsymbol{\phi},\boldsymbol{\omega}_b,\dot{\boldsymbol{\phi}}) & -\mathbf{E}_{3\times3}\end{bmatrix}\begin{bmatrix}\mathbf{a}_d\\\mathbf{L}_0\end{bmatrix}\\&\doteq\bar{\mathbf{Y}}_d\bar{\mathbf{a}}_d\end{aligned}\tag{3}$$

where we call $\bar{\mathbf{Y}}_d=\begin{bmatrix}\mathbf{Y}_d(\boldsymbol{\epsilon}_b,\boldsymbol{\phi},\boldsymbol{\omega}_b,\dot{\boldsymbol{\phi}}) & -\mathbf{E}_{3\times3}\end{bmatrix}$ the generalized dynamic regressor matrix, we call $\bar{\mathbf{a}}_d=\begin{bmatrix}\mathbf{a}_d^{\mathrm{T}} & \mathbf{L}_0^{\mathrm{T}}\end{bmatrix}^{\mathrm{T}}$ the generalized dynamic parameters, $\mathbf{E}_{3\times3}$ is a 3×3 identity matrix, $\boldsymbol{\epsilon}_b\in\mathbb{R}^4$ are quaternions used to represent the spacecraft attitude, and $\mathbf{Y}_d(\boldsymbol{\epsilon}_b,\boldsymbol{\phi},\boldsymbol{\omega}_b,\dot{\boldsymbol{\phi}})\in\mathbb{R}^{3\times p}$ is the regressor matrix.

REMARK 1. The angular momentum conservation law holds for free-floating space manipulators, which illustrates the invariability of the spatial rotation. Bigger angular momentum shows that the FFSM rotates faster around a certain fixed axis. Intuitively, when the initial angular is much bigger, it is difficult to make the manipulator end effector track some desired trajectories in the inertia frame. Hence, bigger initial angular momentum is not desired in practice, and it should be eliminated by the thrusters or other actuators. However, it is inevitable to have some angular momentum for FFSMs in space environments due to some disturbances. In this paper, we assume that the initial angular momentum is small, i.e., the norm of $\mathbf{L}_0$ is small.

B. Kinematics of FFSMs

Denote by m the dimension of the task space. The FFSM end-effector velocity $\dot{\mathbf{x}}\in\mathbb{R}^m$ in the inertial frame can be expressed as [28]

$$\dot{\mathbf{x}}=\mathbf{J}_b\boldsymbol{\omega}_b+\mathbf{J}_m\dot{\boldsymbol{\phi}}+\mathbf{l}_0\tag{4}$$

where $\mathbf{J}_b(\boldsymbol{\epsilon}_b,\boldsymbol{\phi})\in\mathbb{R}^{m\times3}$ and $\mathbf{J}_m(\boldsymbol{\epsilon}_b,\boldsymbol{\phi})\in\mathbb{R}^{m\times n}$ are the Jacobian matrices, and the appearance of the initial translational motion term $\mathbf{l}_0$ is due to the nonzero linear momentum, noting that $\mathbf{l}_0$ is a constant vector.

And the kinematic equation (4) depends linearly on a set of kinematic parameters $\mathbf{a}_k=\begin{bmatrix}a_{k1},a_{k2},\ldots,a_{kj}\end{bmatrix}^{\mathrm{T}}$ and the initial translational motion term $\mathbf{l}_0$ [29], [30]

$$\begin{aligned}\dot{\mathbf{x}}&=\mathbf{J}_b\boldsymbol{\omega}_b+\mathbf{J}_m\dot{\boldsymbol{\phi}}+\mathbf{l}_0\\&=\begin{bmatrix}\mathbf{Y}_k(\boldsymbol{\epsilon}_b,\boldsymbol{\phi},\boldsymbol{\omega}_b,\dot{\boldsymbol{\phi}}) & \mathbf{E}_{3\times3}\end{bmatrix}\begin{bmatrix}\mathbf{a}_k\\\mathbf{l}_0\end{bmatrix}\\&\doteq\bar{\mathbf{Y}}_k\bar{\mathbf{a}}_k\end{aligned}\tag{5}$$

where we call $\bar{\mathbf{Y}}_k=\begin{bmatrix}\mathbf{Y}_k(\boldsymbol{\epsilon}_b,\boldsymbol{\phi},\boldsymbol{\omega}_b,\dot{\boldsymbol{\phi}}) & \mathbf{E}_{3\times3}\end{bmatrix}$ the generalized kinematic regressor matrix, we call $\bar{\mathbf{a}}_k=\begin{bmatrix}\mathbf{a}_k^{\mathrm{T}} & \mathbf{l}_0^{\mathrm{T}}\end{bmatrix}^{\mathrm{T}}$ the generalized kinematic parameters, $\mathbf{Y}_k(\boldsymbol{\epsilon}_b,\boldsymbol{\phi},\boldsymbol{\omega}_b,\dot{\boldsymbol{\phi}})\in\mathbb{R}^{m\times j}$ is called the kinematic regressor matrix.

REMARK 2. In fact, $\mathbf{l}_0$ is the initial velocity of the center of mass of the whole system. The linear momentum conservation law holds for free-floating space manipulators, which illustrates that $\mathbf{l}_0$ is constant. Intuitively, we can see that the end effector of the manipulator can track some desired trajectories in the inertial frame only over a relatively short period of time. What is worse, the FFSM may collide with the target spacecraft if the thrusters or other actuators do not work. Just like the initial angular momentum, the initial linear momentum is also not desired in practice, and it should also be eliminated by the thrusters or other actuators. However, it is also inevitable to have some linear momentum in space environments due to some disturbances. So, in this paper, we assume that the initial linear momentum is small, which means that the norm of $\mathbf{l}_0$ is small.

C. Reaction Null-Space

Following the work of [19], we briefly describe the basic idea of Reaction Null-Space.

The angular momentum equation with zero initial angular momentum $\mathbf{L}=\mathbf{0}$ and zero attitude disturbance $\boldsymbol{\omega}_b=\mathbf{0}$ becomes

$$\bar{\mathbf{H}}_{bm}\dot{\boldsymbol{\phi}}=\mathbf{0}.\tag{6}$$

Equation (6) yields the following null-space solution

$$\dot{\boldsymbol{\phi}}_r=(\mathbf{E}-\bar{\mathbf{H}}_{bm}^{+}\bar{\mathbf{H}}_{bm})\boldsymbol{\zeta}\tag{7}$$

where $(\cdot)^{+}=(\cdot)^{\mathrm{T}}((\cdot)(\cdot)^{\mathrm{T}})^{-1}$ denotes the right pseudoinverse of $(\cdot)$, and noting that $(\cdot)(\cdot)^{+}=\mathbf{E}$, with $\mathbf{E}$ being an identity matrix of proper dimension. The joint motion given by (7) can ensure zero disturbance to the base attitude. The vector $\boldsymbol{\zeta}$ is arbitrary and the null-space of the inertia matrix $\bar{\mathbf{H}}_{bm}\in\mathbb{R}^{3\times n}$ is called the reaction null-space. The expression $\mathbf{P}(\mathbf{q})=\mathbf{E}-\bar{\mathbf{H}}_{bm}^{+}\bar{\mathbf{H}}_{bm}$ appearing in (7) denotes the projector onto the null-space of the coupled inertia matrix $\bar{\mathbf{H}}_{bm}$.

REMARK 3. Eq. (7) can not be linearly parameterized with respect to a set of physical parameters due to the advent of $\bar{\mathbf{H}}_{bm}^{+}$, which is a great challenge to the application of the conventional adaptive control.

In this paper, we assume that there exists the reaction null-space. A necessary condition for the existence of the reaction null-space is the availability of any of the following features: kinematic redundancy, dynamic redundancy, selective reaction null-space, and rank deficiency of the coupled inertia matrix [17].

III. ADAPTIVE REACTIONLESS CONTROL FORMULATION

In this section, we will derive an adaptive reactionless kinematic controller for FFSMs with unknown kinematic and dynamic properties.

A. Problem Formulation

When the dynamic parameters of FFSMs are unknown, we cannot use the control law in (7). Replacing the unknown dynamic parameters $\mathbf{a}_d$ in (7) with their estimates $\hat{\mathbf{a}}_d$, we get the following kinematic control law

$$\dot{\boldsymbol{\phi}}_r^{*}=(\mathbf{E}-\hat{\bar{\mathbf{H}}}_{bm}^{+}\hat{\bar{\mathbf{H}}}_{bm})\boldsymbol{\zeta}\tag{8}$$

where $\hat{\bar{\mathbf{H}}}_{bm}$ is the estimate of the coupled inertia matrix $\bar{\mathbf{H}}_{bm}$.

Hence, the objective of the adaptive reactionless kinematic controller design for FFSM can be stated as: assuming that

there exists a dynamic control law so that $\dot{\boldsymbol{\phi}} \to \dot{\boldsymbol{\phi}}_r^*$ as $t \to \infty$, seek an adaptive kinematic control law which includes the estimated parameters and a parameter adaptation law for updating the estimated parameters to achieve both the attitude regulation of the base spacecraft and continuous path tracking of the manipulator end-effector. That is, $\boldsymbol{\omega}_b \to \mathbf{0}$, $\mathbf{R}_b \to \mathbf{R}_{bd}$, $\Delta\mathbf{x} \to \mathbf{0}$ and $\Delta\dot{\mathbf{x}} \to \mathbf{0}$ as $t \to \infty$. Here, $\Delta\mathbf{x} = \mathbf{x} - \mathbf{x}_d$ is the tracking error of the end-effector, and $\mathbf{x}_d \in \mathbb{R}^m$ is a desired trajectory of the end-effector. The boundedness of $\mathbf{x}_d$, $\dot{\mathbf{x}}_d$, and $\ddot{\mathbf{x}}_d$ is assumed. $\mathbf{R}_b$ and $\mathbf{R}_{bd}$ are the current and desired attitude matrices of the base, respectively. For the attitude regulation problem, the desired attitude matrix $\mathbf{R}_{bd}$ is constant.

REMARK 4. The role of the existing dynamic control law is to make the current joint motion rate track the designed joint motion rate $\dot{\boldsymbol{\phi}}_r^*$ which can be regarded as a reference velocity. Note that, the torque control input does not appear explicitly in (8). However, joint velocity can be achieved by velocity-based closed-loop servo controller straightforwardly based on the work of [31], and thus it can be considered as an input command to the system. Actually, precise velocity control of mechanical system can be easily achieved with the rapid development of mechatronics technology, so it is reasonable to assume that velocity control of robot manipulators can be accomplished with high precision [32].

B. Adaptive Controller Design Considering the Base Attitude Regulation

In order to achieve the attitude regulation of the base spacecraft, the designed joint motion rate in (8) needs to be modified as follows

$$\dot{\boldsymbol{\phi}}_r^* = (\mathbf{E} - \hat{\bar{\mathbf{H}}}_{bm}^+ \hat{\bar{\mathbf{H}}}_{bm})\boldsymbol{\zeta} + \hat{\bar{\mathbf{H}}}_{bm}^+ (\hat{\mathbf{L}}_0 + \hat{\bar{\mathbf{H}}}_b \lambda_b \Delta\boldsymbol{\epsilon}_{bv}) \tag{9}$$

where $\hat{\mathbf{L}}_0$ is the estimate of the initial angular momentum, $\lambda_b > 0$ is a constant, and $\Delta\boldsymbol{\epsilon}_{bv}$ is the vector part of the error quaternion corresponding to the error attitude matrix $\Delta\mathbf{R}_b = \mathbf{R}_{bd}^{\mathrm{T}}\mathbf{R}_b$ [37].

Premultiplying both sides of (9) by $\hat{\bar{\mathbf{H}}}_{bm}$, we have,

$$\hat{\bar{\mathbf{H}}}_{bm}\dot{\boldsymbol{\phi}}_r^* = \hat{\mathbf{L}}_0 + \hat{\bar{\mathbf{H}}}_b \lambda_b \Delta\boldsymbol{\epsilon}_{bv}. \tag{10}$$

Due to the nonzero initial momentum, combining (2) and (10), we get,

$$\hat{\bar{\mathbf{H}}}_{bm}\dot{\boldsymbol{\phi}}_r^* - \hat{\bar{\mathbf{H}}}_b \lambda_b \Delta\boldsymbol{\epsilon}_{bv} - \hat{\mathbf{L}}_0 = \bar{\mathbf{H}}_b\boldsymbol{\omega}_b + \bar{\mathbf{H}}_{bm}\dot{\boldsymbol{\phi}} - \mathbf{L}_0. \tag{11}$$

Subtracting both sides of (11) from $\hat{\bar{\mathbf{H}}}_b\boldsymbol{\omega}_b + \hat{\bar{\mathbf{H}}}_{bm}\dot{\boldsymbol{\phi}}$, we have,

$$\begin{aligned} &\hat{\bar{\mathbf{H}}}_b(\boldsymbol{\omega}_b + \lambda_b\Delta\boldsymbol{\epsilon}_{bv}) + \hat{\bar{\mathbf{H}}}_{bm}(\dot{\boldsymbol{\phi}} - \dot{\boldsymbol{\phi}}_r^*) \\ &= \Delta\bar{\mathbf{H}}_b\boldsymbol{\omega}_b + \Delta\bar{\mathbf{H}}_{bm}\dot{\boldsymbol{\phi}} - \Delta\mathbf{L}_0 \\ &= \begin{bmatrix}\mathbf{Y}_d(\boldsymbol{\epsilon}_b, \boldsymbol{\phi}, \boldsymbol{\omega}_b, \dot{\boldsymbol{\phi}}) & -\mathbf{E}\end{bmatrix}\begin{bmatrix}\Delta\mathbf{a}_d \\ \Delta\mathbf{L}_0\end{bmatrix} \\ &= \bar{\mathbf{Y}}_d\Delta\bar{\mathbf{a}}_d \end{aligned} \tag{12}$$

where $\Delta\bar{\mathbf{H}}_b = \hat{\bar{\mathbf{H}}}_b - \bar{\mathbf{H}}_b$, $\Delta\bar{\mathbf{H}}_{bm} = \hat{\bar{\mathbf{H}}}_{bm} - \bar{\mathbf{H}}_{bm}$, $\Delta\mathbf{L}_0 = \hat{\mathbf{L}}_0 - \mathbf{L}_0$, and $\Delta\bar{\mathbf{a}}_d = \hat{\bar{\mathbf{a}}}_d - \bar{\mathbf{a}}_d$ is the generalized dynamic parameter estimation error. Let

$$\mathbf{y}_1 = \hat{\bar{\mathbf{H}}}_b(\boldsymbol{\omega}_b + \lambda_b\Delta\boldsymbol{\epsilon}_{bv}) + \hat{\bar{\mathbf{H}}}_{bm}(\dot{\boldsymbol{\phi}} - \dot{\boldsymbol{\phi}}_r^*). \tag{13}$$

We assume that the base spacecraft attitude $\boldsymbol{\epsilon}_b$, the angular velocity of the base spacecraft $\boldsymbol{\omega}_b$, the manipulator joint angle $\boldsymbol{\phi}$, and the manipulator joint velocity $\dot{\boldsymbol{\phi}}$ are available from the sensors. Therefore, the signal $\mathbf{y}_1$ is measurable. For the attitude regulation problem, the desired value of $\boldsymbol{\omega}_b$ is zero, and thus the regulation error of the angular velocity of the base spacecraft is $\Delta\boldsymbol{\omega}_b = \boldsymbol{\omega}_b - \mathbf{0} = \boldsymbol{\omega}_b$, which means that $\mathbf{y}_1$ can be rewritten as

$$\mathbf{y}_1 = \hat{\bar{\mathbf{H}}}_b(\Delta\boldsymbol{\omega}_b + \lambda_b\Delta\boldsymbol{\epsilon}_{bv}) + \hat{\bar{\mathbf{H}}}_{bm}(\dot{\boldsymbol{\phi}} - \dot{\boldsymbol{\phi}}_r^*). \tag{14}$$

Now the gradient estimator of the standard form is adopted to update the generalized dynamic parameter estimate $\hat{\mathbf{a}}_d$, and the updating law is given by

$$\dot{\hat{\bar{\mathbf{a}}}}_d = -\boldsymbol{\Gamma}_d\bar{\mathbf{Y}}_d^{\mathrm{T}}\mathbf{y}_1 \tag{15}$$

where $\boldsymbol{\Gamma}_d$ is a diagonal positive definite estimator gain matrix. Based on the work of [33], we know that $\mathbf{y}_1 \in L_2$, and $\hat{\bar{\mathbf{a}}}_d \in L_\infty$.

Differentiating (13) with respect to time, we get,

$$\begin{aligned} \dot{\mathbf{y}}_1 =& \dot{\hat{\bar{\mathbf{H}}}}_b(\boldsymbol{\omega}_b + \lambda_b\Delta\boldsymbol{\epsilon}_{bv}) + \hat{\bar{\mathbf{H}}}_b(\dot{\boldsymbol{\omega}}_b + \lambda_b\Delta\dot{\boldsymbol{\epsilon}}_{bv}) \\ &+ \dot{\hat{\bar{\mathbf{H}}}}_{bm}(\dot{\boldsymbol{\phi}} - \dot{\boldsymbol{\phi}}_r^*) + \hat{\bar{\mathbf{H}}}_{bm}(\ddot{\boldsymbol{\phi}} - \ddot{\boldsymbol{\phi}}_r^*) \end{aligned} \tag{16}$$

where $\ddot{\boldsymbol{\phi}}_r^*$ is the time derivative of $\dot{\boldsymbol{\phi}}_r^*$. We assume that under an existing dynamic control law which can guarantee that $\dot{\boldsymbol{\phi}} \to \dot{\boldsymbol{\phi}}_r^*$ as $t \to \infty$, the entire dynamic system is stable, i.e., $\boldsymbol{\epsilon}_b$, $\boldsymbol{\phi}$, $\boldsymbol{\omega}_b$, $\dot{\boldsymbol{\phi}}$, $\dot{\boldsymbol{\omega}}_b$, and $\ddot{\boldsymbol{\phi}}$ are all bounded. Since the desired attitude matrix of the spacecraft $\mathbf{R}_{bd}$ is constant, the vector part of the error quaternion $\Delta\boldsymbol{\epsilon}_{bv}$ and its derivative $\Delta\dot{\boldsymbol{\epsilon}}_{bv}$ are bounded. It is reasonable to assume that $\boldsymbol{\zeta} \in L_\infty$ and $\dot{\boldsymbol{\zeta}} \in L_\infty$, so (9) leads to that $\dot{\boldsymbol{\phi}}_r^* \in L_\infty$, and from (16), we obtain $\dot{\mathbf{y}}_1 \in L_\infty$, i.e., the signal $\mathbf{y}_1$ is uniformly continuous.

Here, we introduce a sliding variable [37],

$$\mathbf{s}_b = \Delta\boldsymbol{\omega}_b + \lambda_b\Delta\boldsymbol{\epsilon}_{bv}. \tag{17}$$

So far, we have known that $\mathbf{y}_1 \in L_2$ and $\mathbf{y}_1$ is uniformly continuous, and thus $\mathbf{y}_1 \to \mathbf{0}$ as $t \to \infty$ [34]. We assumed that there exists a joint motion control law which can guarantee $\dot{\boldsymbol{\phi}} \to \dot{\boldsymbol{\phi}}_r^*$ as $t \to \infty$. Hence, we obtain, from (14), $\mathbf{s}_b \to \mathbf{0}$ as $t \to \infty$ if $\hat{\bar{\mathbf{H}}}_b$ is uniformly positive definite.

According to the analysis in the work of [37], the fact that $\mathbf{s}_b \to \mathbf{0}$ as $t \to \infty$ implies that $\Delta\boldsymbol{\epsilon}_{bv} \to \mathbf{0}$ and $\Delta\boldsymbol{\omega}_b \to \mathbf{0}$ as $t \to \infty$, which means that $\boldsymbol{\omega}_b \to \mathbf{0}$ and $\mathbf{R}_b \to \mathbf{R}_{bd}$ as $t \to \infty$.

REMARK 5. Here we assume that the estimate of the inertia matrix of the base $\hat{\bar{\mathbf{H}}}_b$ is positive definite, which can be guaranteed by the parameter projection algorithm [35], [36].

Now, summarizing the above analysis, we will state the following theorem.

Theorem 1: The kinematic control law (9) and the parameter adaptation law (15) achieve the base attitude regulation provided that there exists a dynamic control law so that $\dot{\boldsymbol{\phi}} \to \dot{\boldsymbol{\phi}}_r^*$ as $t \to \infty$. That is, $\boldsymbol{\omega}_b \to \mathbf{0}$ and $\mathbf{R}_b \to \mathbf{R}_{bd}$ as $t \to \infty$.

C. Adaptive Controller Design Considering Both the Base Attitude Regulation and Continuous Path Tracking

When FFSMs are executing OOS, it is usually not enough to control only the attitude of the base spacecraft. Under this circumstance, the end-effector of the FFSM is usually required to track a desired trajectory $\mathbf{x}_d \in \mathbb{R}^m$. Here, we assume that the space manipulator is operating in a workspace where the dynamic singularity does not occur.

Let d_1 and $d_2(=m)$ be the number of task variables for the spacecraft task and the end-effector task, respectively. As long as the number of the manipulator joints n is not smaller than the total number of task variables d_1+d_2, i.e., $n \geq d_1+d_2$, the base attitude regulation and simultaneous continuous path tracking of the end-effector will be achieved by making appropriate choice of $\boldsymbol{\zeta}$ [16]. So $n \geq d_1+d_2$ is assumed in this paper.

Next, we will exploit the property of $\boldsymbol{\zeta}$ to achieve both the base attitude regulation and continuous path tracking.

If the parameters of the FFSM are exactly known, for the task of continuous path tracking with simultaneous spacecraft attitude maintenance, $\boldsymbol{\zeta}$ is designed as [16],

$$\boldsymbol{\zeta} = (\mathbf{J}_m(\mathbf{E} - \bar{\mathbf{H}}_{bm}^{+}\bar{\mathbf{H}}_{bm}))^{+}\dot{\mathbf{x}}_d. \tag{18}$$

When both the generalized dynamic parameters and the generalized kinematic parameters are unknown, we propose the following kinematic control law

$$\dot{\boldsymbol{\phi}}_r^{*} = (\mathbf{E} - \hat{\bar{\mathbf{H}}}_{bm}^{+}\hat{\bar{\mathbf{H}}}_{bm})\boldsymbol{\zeta} + \hat{\bar{\mathbf{H}}}_{bm}^{+}(\hat{\bar{\mathbf{L}}}_0 + \hat{\bar{\mathbf{H}}}_b\lambda_b\Delta\boldsymbol{\epsilon}_{bv}) \tag{19}$$

where

$$\boldsymbol{\zeta} = (\hat{\mathbf{J}}_m\hat{\mathbf{P}})^{+}[-\hat{\mathbf{l}}_0 + \dot{\mathbf{x}}_d - \boldsymbol{\Lambda}_x\Delta\mathbf{x} - \hat{\mathbf{J}}_m\hat{\bar{\mathbf{H}}}_{bm}^{+}(\hat{\bar{\mathbf{L}}}_0 + \hat{\bar{\mathbf{H}}}_b\lambda_b\Delta\boldsymbol{\epsilon}_{bv})] \tag{20}$$

and $\boldsymbol{\Lambda}_x$ is a constant symmetric positive definite matrix.

Since the new control law (19) is a special case of the previous control law (9), (19) will certainly ensure the base attitude regulation. Next, we will show that (19) can also achieve continuous path tracking of the end-effector.

Premultiplying both sides of (19) by $\hat{\mathbf{J}}_m$, we get,

$$\hat{\mathbf{J}}_m\dot{\boldsymbol{\phi}}_r^{*} = \dot{\mathbf{x}}_d - \boldsymbol{\Lambda}_x\Delta\mathbf{x} - \hat{\mathbf{l}}_0. \tag{21}$$

Combining (4) and (21), we have,

$$\dot{\mathbf{x}}_d - \boldsymbol{\Lambda}_x\Delta\mathbf{x} - \hat{\mathbf{J}}_m\dot{\boldsymbol{\phi}}_r^{*} - \hat{\mathbf{l}}_0 = \dot{\mathbf{x}} - \mathbf{J}_b\boldsymbol{\omega}_b - \mathbf{J}_m\dot{\boldsymbol{\phi}} - \mathbf{l}_0. \tag{22}$$

Adding $\hat{\mathbf{J}}_b\boldsymbol{\omega}_b + \hat{\mathbf{J}}_m\dot{\boldsymbol{\phi}}$ to both sides of (22), and after some simple calculations, we obtain,

$$\hat{\mathbf{J}}_b\boldsymbol{\omega}_b + \hat{\mathbf{J}}_m(\dot{\boldsymbol{\phi}} - \dot{\boldsymbol{\phi}}_r^{*}) - (\Delta\dot{\mathbf{x}} + \boldsymbol{\Lambda}_x\Delta\mathbf{x}) = \Delta\mathbf{J}_b\boldsymbol{\omega}_b + \Delta\mathbf{J}_m\dot{\boldsymbol{\phi}} + \Delta\mathbf{l}_0 \tag{23}$$

where $\Delta\mathbf{J}_b = \hat{\mathbf{J}}_b - \mathbf{J}_b$, $\Delta\mathbf{J}_m = \hat{\mathbf{J}}_m - \mathbf{J}_m$, and $\Delta\mathbf{l}_0 = \hat{\mathbf{l}}_0 - \mathbf{l}_0$. From (5), the right hand side of (23) can be linearly parameterized, so we get,

$$\underbrace{\hat{\mathbf{J}}_b\boldsymbol{\omega}_b + \hat{\mathbf{J}}_m(\dot{\boldsymbol{\phi}} - \dot{\boldsymbol{\phi}}_r^{*}) - (\Delta\dot{\mathbf{x}} + \boldsymbol{\Lambda}_x\Delta\mathbf{x})}_{\mathbf{y}_2} = \bar{\mathbf{Y}}_k(\boldsymbol{\epsilon}_b, \boldsymbol{\phi}, \boldsymbol{\omega}_b, \dot{\boldsymbol{\phi}})\Delta\bar{\mathbf{a}}_k \tag{24}$$

where $\Delta\bar{\mathbf{a}}_k = \hat{\bar{\mathbf{a}}}_k - \bar{\mathbf{a}}_k$ is the generalized kinematic parameter estimation error. We assume that the position and the velocity of the end-effector are available from certain sensors. Hence, the signal $\mathbf{y}_2$ is measurable. And the kinematic parameter estimates are updated by

$$\dot{\hat{\bar{\mathbf{a}}}}_k = -\boldsymbol{\Gamma}_k\bar{\mathbf{Y}}_k^{\mathrm{T}}\mathbf{y}_2 \tag{25}$$

where $\boldsymbol{\Gamma}_k$ is a diagonal positive definite estimator gain matrix. Here, we introduce another sliding variable [38],

$$\mathbf{s}_x = \Delta\dot{\mathbf{x}} + \boldsymbol{\Lambda}_x\Delta\mathbf{x}. \tag{26}$$

Because the new kinematic controller (19) with the gradient estimator (15) has all the properties which the previous kinematic controller (9) with the same kind of estimator bears, thus, we know that $\hat{\bar{\mathbf{a}}}_d \in L_\infty$, and $\boldsymbol{\omega}_b \to \mathbf{0}$ as $t \to \infty$. Due to the property of the gradient estimator [33], we conclude that $\hat{\bar{\mathbf{a}}}_k \in L_\infty$ and $\mathbf{y}_2 \in L_2$. And also we assume that the whole system is stable under an exiting dynamic control law guaranteeing that $\dot{\boldsymbol{\phi}} \to \dot{\boldsymbol{\phi}}_r^{*}$ as $t \to \infty$, i.e., $\boldsymbol{\epsilon}_b$, $\boldsymbol{\phi}$, $\boldsymbol{\omega}_b$, $\dot{\boldsymbol{\phi}}$, $\dot{\boldsymbol{\omega}}_b$, and $\ddot{\boldsymbol{\phi}}$ are all bounded, so the end-effector position in the inertial frame is also bounded from the forward kinematics, and it implies that both $\dot{\mathbf{x}}$ and $\ddot{\mathbf{x}}$ are bounded from the kinematic equation (4). Thus (19) gives that $\dot{\boldsymbol{\phi}}_r^{*} \in L_\infty$. Hence, $\dot{\mathbf{y}}_2$ is bounded, which means that $\mathbf{y}_2$ is uniformly continuous. The fact that $\mathbf{y}_2 \in L_2$ and $\mathbf{y}_2$ is uniformly continuous leads to that $\mathbf{y}_2 \to \mathbf{0}$ as $t \to \infty$ [34]. Since we have had $\boldsymbol{\omega}_b \to \mathbf{0}$ and $\dot{\boldsymbol{\phi}} \to \dot{\boldsymbol{\phi}}_r^{*}$ as $t \to \infty$, the definition of $\mathbf{y}_2$ means that $\mathbf{s}_x \to \mathbf{0}$ as $t \to \infty$.

According to the analysis in the work of [38], $\mathbf{s}_x \to \mathbf{0}$ as $t \to \infty$ implies that $\Delta\mathbf{x} \to \mathbf{0}$ and $\Delta\dot{\mathbf{x}} \to \mathbf{0}$ as $t \to \infty$, which means that $\mathbf{x} \to \mathbf{x}_d$ and $\dot{\mathbf{x}} \to \dot{\mathbf{x}}_d$ as $t \to \infty$.

Now, summarizing the above analysis, we have the following theorem.

Theorem 2: The kinematic control law (19) and the parameter adaptation laws (15), (25) achieve the base attitude regulation and the convergence of the FFSM end-effector tracking errors provided that there exists a dynamic control law so that $\dot{\boldsymbol{\phi}} \to \dot{\boldsymbol{\phi}}_r^{*}$ as $t \to \infty$. That is, $\boldsymbol{\omega}_b \to \mathbf{0}$, $\mathbf{R}_b \to \mathbf{R}_{bd}$, $\Delta\mathbf{x} \to \mathbf{0}$ and $\Delta\dot{\mathbf{x}} \to \mathbf{0}$ as $t \to \infty$.

IV. SIMULATION RESULTS

In this section we present simulation results for the proposed adaptive control law via a three-DOF planar space manipulator (Fig. 1). The base attitude regulation and simultaneous trajectory tracking of the end-effector in task space is required. We assume that the velocity servo control is fast enough so that the designed joint motion rate $\dot{\boldsymbol{\phi}}_r^{*}$ can be tracked very quickly, so in the simulation $\dot{\boldsymbol{\phi}} = \dot{\boldsymbol{\phi}}_r^{*}$ holds.

For the system considered here, the number of the manipulator joints $n = 3$, and the number of task variables for the spacecraft task is $d_1 = 1$. If we are interested in the position and the linear velocity of the end-effector, the number of task variables for the end-effector task $d_2 = 2$. Thus, $n = d_1 + d_2$, which implies that the available redundancy can be utilized only to coordinate the end-effector-spacecraft motion, so in this simulation the attitude of the base spacecraft is required to be regulated to a desired state, meanwhile, the FFSM end-effector is required to track a desired trajectory in the task space. Without loss of generality, the desired value of the base attitude is assumed to be zero, i.e, $q_{bd} = 0$.

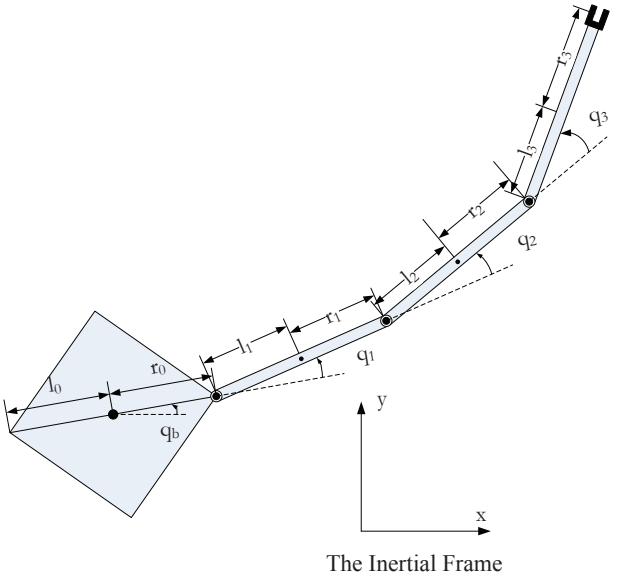

Fig. 1. A three-DOF planar space manipulator.

TABLE I
THE MANIPULATOR PARAMETERS

i-th body	m_i(kg)	I_i(kg · m^2)	l_i(m)	r_i(m)
0	60.0	11.2500	0.75	0.75
1	6.0	1.1250	0.75	0.75
2	5.0	0.9375	0.75	0.75
3	5.0	0.9375	0.75	0.75

The physical parameters of the space manipulator are listed in Table I, where m_i and I_i $(i = 0, 1, 2, 3)$ are the mass and moment of inertia of the i-th rigid body about the center of mass, respectively, l_i and r_i are shown as Fig. 1, and the 0-th body denotes the base spacecraft. The sampling period used in the following simulations is 2ms.

Matrix expressions for $\bar{\mathbf{H}}_b$, $\bar{\mathbf{H}}_{bm}$, $\mathbf{J}_b$, and $\mathbf{J}_m$ can be found in [39]. And the kinematic parameters and dynamic parameters are listed in Appendix.

In simulations, the desired end-effector trajectory of the 3-DOF FFSM is a circle in inertial space which is given by

$$\mathbf{x}_d = \begin{bmatrix} 3.7 + 0.3\cos(\pi t) \\ 0.2 + 0.3\sin(\pi t) \end{bmatrix}.$$

The initial state of the 3-DOF space manipulator is as follows: the position of the center of mass of the spacecraft is $\mathbf{R}_{C0} = \begin{bmatrix} 0 & 0 \end{bmatrix}^{\mathrm{T}}$, the initial configuration of the FFSM is $\mathbf{q}(0) = \begin{bmatrix} 0 & \pi/3 & -2\pi/3 & \pi/3 \end{bmatrix}^{\mathbf{T}}$ and the initial position of the FFSM end-effector is $\mathbf{x}_0 = \begin{bmatrix} 3.75 & 0 \end{bmatrix}^{\mathrm{T}}$. The FFSM is not initially at rest and the initial velocities are set as $\dot{\mathbf{R}}_{C0} = \begin{bmatrix} 0.1 & 0.1 \end{bmatrix}^{\mathrm{T}}$, and $\dot{\mathbf{q}}(0) = \begin{bmatrix} -0.05 & 0.05 & 0.05 & 0.05 \end{bmatrix}^{\mathbf{T}}$. The initial values of the generalized kinematic and dynamic parameter estimates are chosen as

$$\hat{\mathbf{a}}_k(0) = \begin{bmatrix} 2 & 3 & 3 & 3 & 0 & 0 \end{bmatrix}^{\mathrm{T}},$$

$$\hat{\mathbf{a}}_d(0) = \begin{bmatrix} 30 & 20 & 3 & 3 & 3 & 5 & 100 & 50 & 30 & 2 & 0 \end{bmatrix}^{\mathrm{T}}.$$

The actual values of the kinematic parameter and dynamic parameter are obtained based on the physical parameters given in Table I,

$$\mathbf{a}_k = \begin{bmatrix} 0.5921 & 1.2434 & 1.3520 & 1.4507 & 0.1 & 0.1 \end{bmatrix}^{\mathrm{T}},$$

$$\mathbf{a}_d = [11.5461 \quad 13.9885 \quad 4.6628 \quad 5.0699 \quad 6.6612 \quad 2.2204 \quad 57.2516 \quad 38.8964 \quad 16.8997 \quad 3.5650 \quad 3.7500]^{\mathrm{T}}.$$

The actual value of the initial angular momentum is $\mathbf{L}_0 = 0.1915$, and the actual value of $\mathbf{l}_0$ is $\mathbf{l}_0 = \begin{bmatrix} 0.1064 & 0.1007 \end{bmatrix}^{\mathrm{T}}$.

The design parameters of the proposed controller are determined as $\mathbf{\Gamma}_d = \mathrm{diag}([30 \ 30 \ 10 \ 10 \ 10 \ 10 \ 10 \ 10 \ 10 \ 10 \ 1])$, $\mathbf{\Gamma}_k = \mathrm{diag}([20 \ \ 20 \ \ 20 \ \ 20 \ \ 2 \ \ 2])$.

If we use the previous controller (19) in our work [23], i.e., the effects of the nonzero initial linear and angular momenta are not considered in the controller (19), the performance of the previous controller is shown in Figs. 2-4.

By contrast, the performance will be improved if the new controller (19) proposed in this paper is adopted. Under the circumstances, we estimate both the generalized dynamic parameters $\bar{\mathbf{a}}_d$ and the generalized kinematic parameters $\bar{\mathbf{a}}_k$, taking into consideration the nonzero initial momenta. The simulation results of the proposed adaptive controller are shown in Figs. 5-12. Fig. 5 and 6 shows the angular velocity

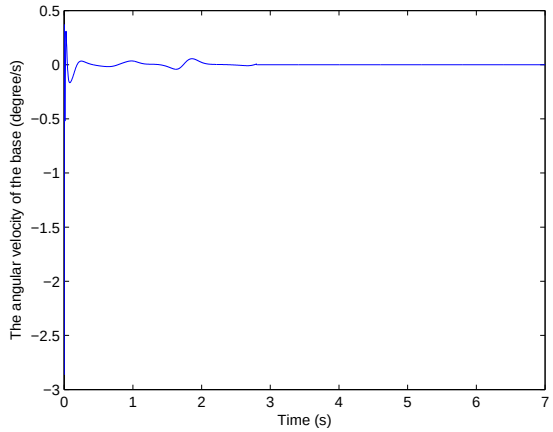

Fig. 2. The angular velocity of the base spacecraft (the previous controller).

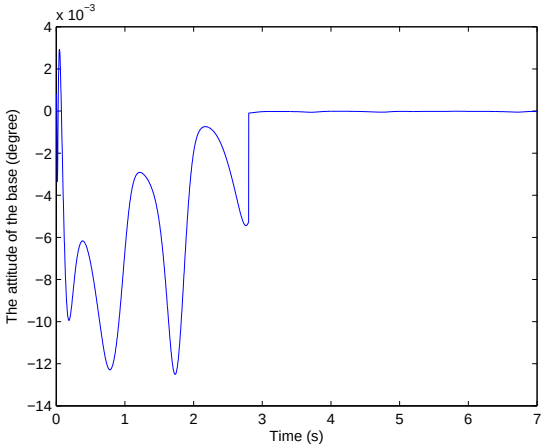

Fig. 3. The attitude of the base spacecraft (the previous controller).

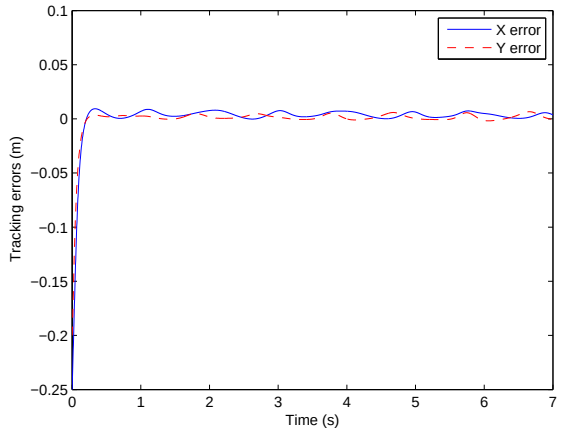

Fig. 4. FFSM end-effector tracking errors (the previous controller).

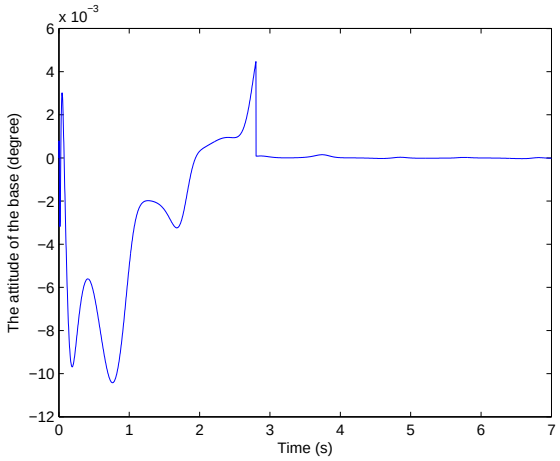

Fig. 6. The attitude of the base spacecraft (the new controller).

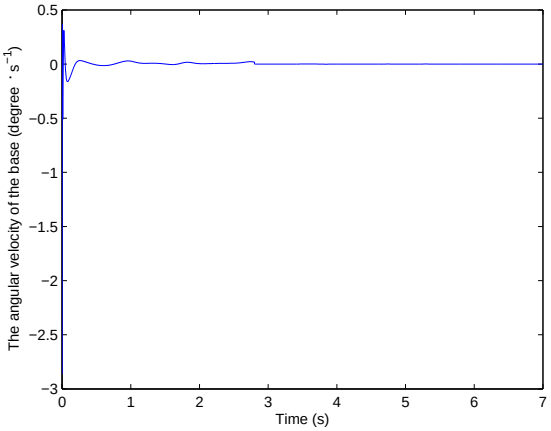

Fig. 5. The angular velocity of the base spacecraft (the new controller).

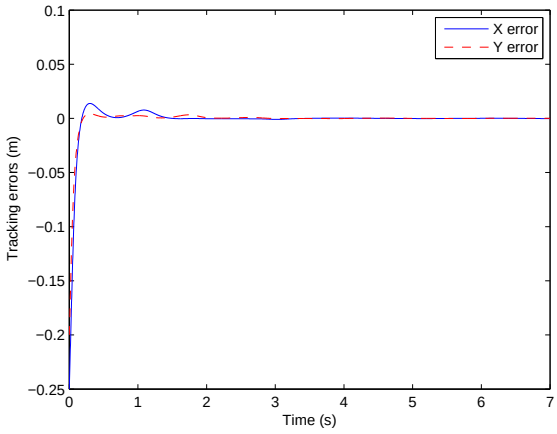

Fig. 7. FFSM end-effector tracking errors (the new controller).

and the attitude of the base. Fig. 7 gives the FFSM end-effector tracking errors.

Since the magnitude of the initial angular momentum and the initial velocity of the FFSM are rather smaller compared with that of the dynamic parameters and the kinematic parameters, for clarity, we shall not present the estimates of the generalized dynamic parameters and that of the generalized kinematic parameters in one figure, respectively. Instead, the estimates of the initial angular momentum and the initial velocity of the FFSM are given in Fig. 9 and Fig. 11. Fig. 8 and Fig. 10 show the dynamic and kinematic parameter estimates, respectively. Fig. 12 describes the desired and actual paths of the FFSM end-effector. Fig. 13 presents the estimation of the inertia matrix $\mathbf{H}_b$.

Fig. 5 shows that the angular velocity of the base spacecraft tends to zero as time evolves. From Fig. 6, we see that the attitude of the base spacecraft tends to zero which is the desired value. Compared with their counterpart, no significant differences were made when we investigate the convergence of the base angular velocity and the base attitude. However, the difference lies in the tracking error of the end-effector. As seen from Fig. 4, large tracking errors are induced due to the

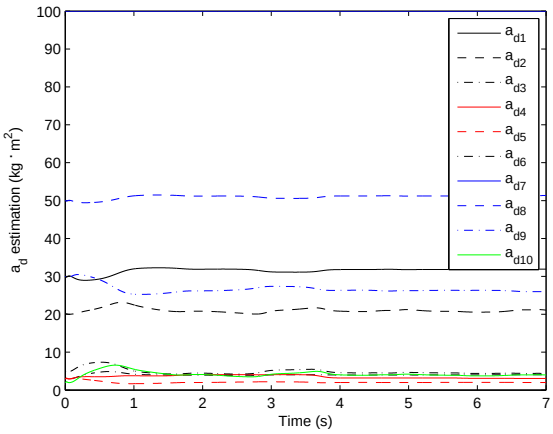

Fig. 8. The dynamic parameter estimates.

nonzero momenta. The comparison between them illustrates the effectiveness the new controller. Fig. 13 shows that the estimated inertia of the base spacecraft is always positive definite (here, $\hat{\mathbf{H}}_b$ is a 1×1 matrix), so the parameter projection algorithm is not required here.

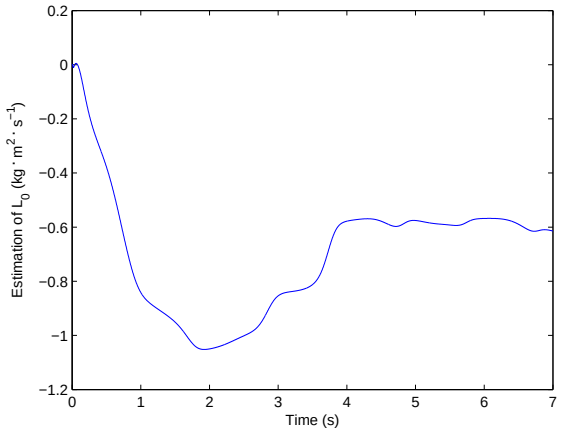

Fig. 9. Estimation of the initial angular momentum $\mathbf{L}_0$.

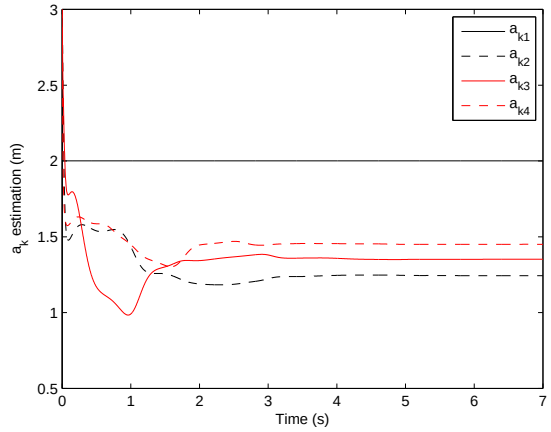

Fig. 10. The kinematic parameter estimates.

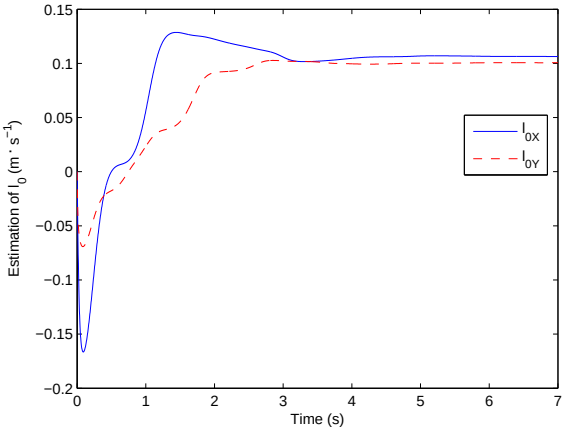

Fig. 11. Estimation of the initial velocity of the FFSM $\mathbf{l}_0$.

To illustrate the convergence of the proposed controller, in the simulation, we give a desired trajectory that initially deviates from the end-effector position, as shown in Fig. 7 and 12 and as time evolves the end-effector approaches the desired trajectory.

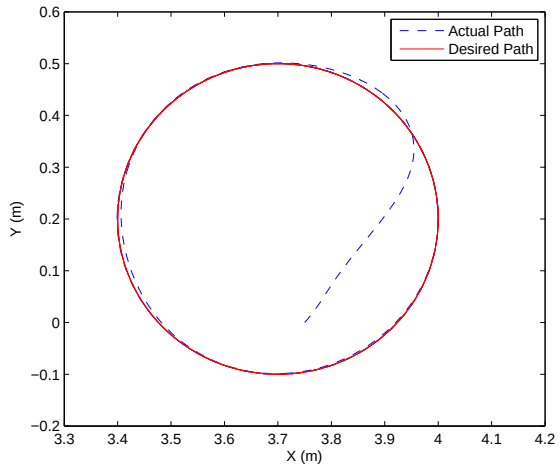

Fig. 12. The actual and desired paths of FFSM end-effector (the new controller).

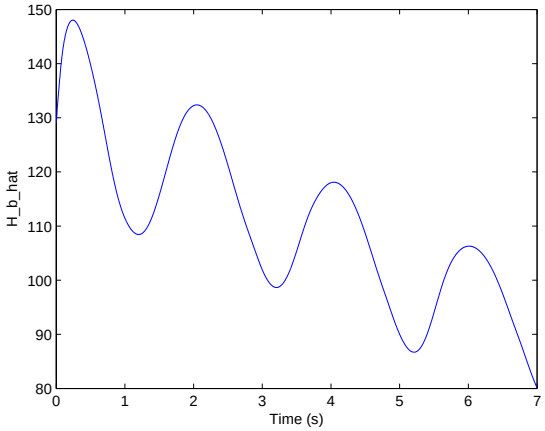

Fig. 13. Estimation of $\mathbf{H}_b$.

V. Conclusion

In this paper, we have developed an adaptive version of RNS-based control for free-floating space manipulators with uncertain kinematics and dynamics in the presence of nonzero initial angular and linear momenta. We skillfully obtain a linear expression which is crucial to estimate the unknown parameters, based on which, we then proposed an adaptive reactionless joint motion controller at velocity level. By exploiting the feature of the vector $\boldsymbol{\zeta}$, the controller can guarantee that the end-effector tracks the desired path in inertial space and meanwhile the attitude regulation of the base spacecraft can be accomplished. It is worth noting that the adaptive controller can also deal with the capture of an unknown target from which uncertainties arise. Next, we will develop the adaptive reactionless joint motion control law at acceleration level, which will be our future work.

APPENDIX

The kinematic parameters $\mathbf{a}_k = \left[a_{k1}, a_{k2}, \ldots, a_{kj}\right]^{\mathrm{T}}$ are listed as follows:

$$
\begin{aligned}
a_{k1} &= m_0 r_0 / M, \\
a_{k2} &= [m_0(l_1 + r_1) + m_1 r_1]/M, \\
a_{k3} &= [(m_0 + m_1)(l_2 + r_2) + m_2 r_2]/M, \\
a_{k4} &= [(m_0 + m_1 + m_2)(l_3 + r_3) + m_3 r_3]/M,
\end{aligned}
$$

and the dynamic parameters

$$\mathbf{a}_d = \left[a_{d1}, a_{d2}, a_{d3}, a_{d4}, a_{d5}, a_{d6}, a_{d7}, a_{d8}, a_{d9}, a_{d10}\right]^{\mathrm{T}}$$

are listed as follows:

$$
\begin{aligned}
a_{d1} &= M_0 r_0 l_1 + M_1 r_0 r_1, \\
a_{d2} &= M_1 l_1 l_2 + M_2 l_1 r_2 + M_3 r_1 l_2 + M_4 r_1 r_2, \\
a_{d3} &= M_2 l_1 l_3 + M_4 r_1 l_3, \\
a_{d4} &= M_4 l_2 l_3 + M_5 r_2 l_3, \\
a_{d5} &= M_1 r_0 l_2 + M_2 r_0 r_2, \\
a_{d6} &= M_2 r_0 l_3, \\
a_{d7} &= J_0 + J_1 + J_2 + J_3, \\
a_{d8} &= J_1 + J_2 + J_3, \\
a_{d9} &= J_2 + J_3, \\
a_{d10} &= J_3,
\end{aligned}
$$

where

$$
\begin{aligned}
M_0 &= m_0(m_1 + m_2 + m_3)/M, \\
M_1 &= m_0(m_2 + m_3)/M, \\
M_2 &= m_0 m_3 / M, \\
M_3 &= (m_0 + m_1)(m_2 + m_3)/M, \\
M_4 &= m_3(m_0 + m_1)/M, \\
M_5 &= m_3(m_0 + m_1 + m_2)/M, \\
M &= m_0 + m_1 + m_2 + m_3, \\
J_0 &= I_0 + M_0 r_0^2, \\
J_1 &= I_1 + M_0 l_1^2 + M_3 r_1^2 + 2 M_1 l_1 r_1, \\
J_2 &= I_2 + M_3 l_2^2 + M_5 r_2^2 + 2 M_4 l_2 r_2, \\
J_3 &= I_3 + M_5 l_3^2.
\end{aligned}
$$

ACKNOWLEDGMENT

The authors would like to thank Dr. Yong Wang and Dr. Xindong Li for their suggestions on improving the quality of this paper.

REFERENCES

[1] Stoll, E., Letschnik, J., Walter, U., Artigas, J., Kremer, P., Preusche, C., and Hirzinger, G. On-orbit servicing. *IEEE Robotics and Automation Magazine*, **16**, 4(2009), 29-33.

[2] Imaida, T., Yokokohji, Y., Doi, T., Oda, M., and Yoshikawa, T. Ground-space bilateral teleoperation experiment using ETS-VII robot arm with direct kinesthetic coupling. In *Proceedings of the IEEE International Conference on Robotics and Automation*, Seoul, Korea, 2001, pp. 1031-1038.

[3] G. Hirzinger and K. Landzettel and B. Brunner and M. Fischer and C. Preusche and D. Reintsema and A. Albu-Schäffer and G. Schreiber and B.-M. Steinmetz. DLR's robotics technologies for on-orbit servicing. *Advanced Robotics*, **18**, 2(2004), 139-174.

[4] Weismuller, T. and Leinz, M. GN&C technology demonstrated by the orbital express autonomous rendezvous and capture sensor system. In *Proceedings of the 29th AAS Guidance and Control Conference*, Breckenridge, CO, USA, 2006, pp. 1-9.

[5] Slotine, J.-J. E. and Li, W. Composite adaptive control of robot manipulators. *Automatica*, **25**, 4(1989), 509-519.

[6] Wang H. and Xie, Y. Prediction error based adaptive Jacobian tracking for free-floating space manipulators. *IEEE Transactions on Aerospace and Electronic Systems*, **48**, 4(2012), 3207-3221.

[7] Papadopoulos, E. (1990). On the dynamics and control of space manipulators. *Ph.D. Thesis*, Dept. of Mechanical Engineering, Massachusetts Institute of Technology, Cambridge, MA.

[8] Aghili, F. Coordination control of a free-flying manipulator and its base attitude to capture and detumble a noncooperative satellite. In *Proceedings of the IEEE/RSJ International Conference on Intelligent Robots and Systems*, St. Louis, USA, 2009, pp. 2365-2372.

[9] Vafa, Z. and Dubowsky, S. On the dynamics of space manipulators using the virtual manipulator, with applications to path planning. *The Journal of the Astronautical Sciences*, **38**, 4(1990), 441-472.

[10] Nakamura, Y. and Mukherjee, R. Nonholonomic path planning of space robots via a bidirectional approach. *IEEE Transanctions on Robots and Automation*, **7**, 4(1991), 500-514.

[11] Fernandes, C., Gurvits, L., and Li, Z. Near-optimal nonholonomic motion planning for a system of coupled rigid bodies. *IEEE Transanctions on Automatic Control*, **39**, 3(1994), 450-463.

[12] Dubowsky, S. and Torres, M. Path planning for space manipulators to minimize spacecraft attitude disturbances. In *Proceedings of the IEEE International Conference on Robotics and Automation*, Sacramento, California, USA, 1991, pp. 2522-2528.

[13] Yamada, K. Arm path planning for a space robot. In *Proceedings of the IEEE/RSJ International Conference on Intelligent Robots and Systems*, Yokohama, Japan, 1993, pp. 2049-2055.

[14] Suzuki, T. and Nakamura, Y. Planning spiral motion of nonholonomic space robots. In *Proceedings of the IEEE International Conference on Robotics and Automation*, Minneapolis, Minnesota, USA, 1996, pp. 718-725.

[15] Tortopidis, I. and Papadopoulos, E. On point-to-point motion planning for underactuated space manipulator systems. *Robotics and Autonomous Systems*, **55**, 2(2007), 122-131.

[16] Nenchev, D., Umetani, Y., and Yoshida, K. Analysis of a redundant free-flying spacecraft/manipulator system. *IEEE Transactions on Robotics and Automation*, **8**, 1(1992), 1-6.

[17] Nenchev, D., Yoshida, K., Vichitkulsawat, P., and Uchiyama, M. Reaction null-space control of flexible structure mounted manipulator systems. *IEEE Transactions on Robotics and Automation*, **15**, 6(1999), 1011-1023.

[18] Yoshida, K., Hashizume, K., and Abiko, S. Zero Reaction Maneuver: flight validation with ETS-VII space robot and extension to kinematically redundant arm. In *Proceedings of the IEEE International Conference on Robotics and Automation*, Seoul, Korea, 2001, pp. 441-446.

[19] Yoshida, K. Engineering Test Satellite VII flight experiments for space robot dynamics and control: theories on laboratory test beds ten years ago, now in orbit. *The International Journal of Robotics Research*, **22**, 5(2003), 321-335.

[20] Fukazu, Y., Hara, N., Kanamiya, Y., and Sato, D. Reactionless resolved acceleration control with vibration suppression capability for JEMRMS/SFA. In *Proceedings of the IEEE International Conference on Robotics and Biomimetics*, Bankok, Thailand, 2009, pp. 1359-1364.

[21] Piersigilli, P., Sharf, I., and Misra A. K. Reactionless capture of a satellite by a two degree-of-freedom manipulator. *Acta Astronautica*, **66**, 1-2(2010), 183-192.

[22] Nguyen Huynh, T. C. and Sharf, I. Adaptive reactionless motion and parameter identification in post-capture of space debris. *Journal of Guidance, Control, and Dynamics*, **36**, 2(2013), 404-414.

[23] Xu, S., Wang, H., Zhang, D., and Yang, B. Adaptive reactionless motion control for free-floating space manipulators with uncertain kinematics and dynamics. In *Proceedings of the 3rd IFAC International Conference on Intelligent Control and Automation Science*, Chengdu, China, 2013, pp. 524-531.

[24] Xu, Y., Shum, H.-Y., Lee, J.-J., and Kanade, T. Adaptive control of space robot system with an attitude controlled base. In *Proceedings of IEEE*

International Conference on Robotics and Automation, Nice, France, 1992, pp. 2005-2010.
[25] Xu, Y., Shum, H.-Y., Kanade, T., and Lee, J.-J. Parameterization and adaptive control of space robot systems. *IEEE Transactions on Aerospace and Electronic Systems*, **30**, 2(1994), 435-451.
[26] Yoshida, K. Practical coordination control between satellite attitude and manipulator reaction dynamics based on computed momentum concept. In *Proceedings of the IEEE/RSJ/GI International Conference on Intelligent Robots and Systems, and 'Advanced Robotic Systems and the Real World'*, Munich, Germany, 1994, pp. 1578-1585.
[27] Abiko, S. and Hirzinger, G. An adaptive control for a free-floating space robot by using inverted chain approach. In *Proceedings of the IEEE/RSJ International Conference on Intelligent Robots and Systems*, San Diego, CA, USA, 2007, pp. 2236-2241.
[28] Umetani, Y. and Yoshida, K. Resolved motion rate control of space manipulators with generalized Jacobian matrix. *IEEE Transactions on Robotics and Automation*, **5**, 3(1989), 303-314.
[29] Ma, B. and Huo, W. Adaptive control of space robot system with an attitude controlled base. In *Proceedings of the IEEE International conference on Robotics and Automation*, Nagoya, Japan, 1995, pp. 1265-1270.
[30] Cheah, C. C., Liu, C., and Slotine, J.-J. E. Approximate Jacobian adaptive control for robot manipulators. In *Proceedings of the IEEE International Conference on Robotics and Automation*, New Orleans, USA, 2004, pp. 3075-3080.
[31] Konno, A., Uchiyama, M., Kito, Y., and Murakami, M. Configuration-dependent vibration controllability of flexible-link manipulators. *The International Journal of Robotics Research*, **16**, 4(1997), 567-576.
[32] Sagara, S., Hideura, M., Katoh, R., Yamashita, T., Kobayashi, J., and Ohkawa, F. Adaptive RMRC for cooperative manipulation of a floating object by two free-based space robots. In *Proceedings of the IEEE/RSJ International Conference on Intelligent Robots and Systems*, Victoria, B.C., Canada, 1998, pp. 1467-1472.
[33] Slotine, J.-J. E. and Li, W. *Applied nonlinear control*. Englewood Cliffs, NJ: Prentice Hall, 1991.
[34] Desoer, C. A. and Vidyasagar, M. *Feedback systems: input-output properties*. New York: Academic Press, 1975.
[35] Ioanou, P. A. and Sun, J. *Robust adaptive control*. Upper Saddle River, NJ: Prentice Hall, 1996.
[36] Wang, H. and Xie, Y. On the uniform positive definiteness of the estimated inertia for robot manipulators. In *Proceedings of the 18th IFAC World Congress*, Milano, Italy, 2011, pp. 4089-4094.
[37] Egeland, O. and Godhavn, J.-M. Passivity-based adaptive attitude control of a rigid spacecraft. *IEEE Transactions on Automatic Control*, **39**, 4(1994), 842-846.
[38] Slotine, J.-J. E. and Li, W. On the adaptive control of robot manipulators. *The International Journal of Robotics Research*, **6**, 3(1987), 49-59.
[39] Nenchev, D., Yoshida, K., and Umentani, Y. Introduction of redundant arms for manipulation in space. In *Proceedings of the IEEE International Workshop on Intelligent Robots*, Tokyo, Japan, 1988, pp. 679-684.

Shuanfeng Xu was born in China in 1983. He received his M.S. degree in control theory and control engineering from Shanghai Jiao Tong University, China, in 2010. Since 2010, he has been with Beijing Institute of Control Engineering, China Academy of Space Technology to pursue his Ph.D. His research interests focus on dynamics, adaptive control of robotic manipulators and space manipulators.

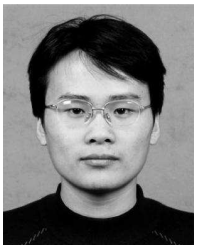

Hanlei Wang received the B.S. degree in Mechanical Engineering from Shijiazhuang Railway Institute, China, in 2004, the M.S. degree in Mechanical Engineering from Harbin Institute of Technology, China, in 2006, and the Ph.D. degree in Control Theory and Control Engineering from Beijing Institute of Control Engineering, China Academy of Space Technology, China, in 2009.

He joined Beijing Institute of Control Engineering as an Engineer in 2009. Since 2011, he has been a Senior Engineer in Beijing Institute of Control Engineering. His research interests include robotics, spacecraft, networked systems, teleoperation, and nonlinear control.

Duzhou Zhang received the M.S. degree in control theory and its applications from Harbin Institute of Technology, China, in 1993. Since 1993, he has been with Beijing Institute of Control Engineering, China Academy of Space Technology. His research interests focus on guidance, navigation and control of spacecraft. He is now a director of Chinese Society of Space Research and Chinese Society of Astronautics.

Baohua Yang received the B.S. degree from Tsinghua University, China, in 1985, the M.S. degree from Beijing Institute of Control Engineering, China Academy of Space Technology, China, in 1988, and the Ph.D. degree in Control Theory and Control Engineering from Harbin Institute of Technology, China, in 2006. From 1988 to 1995 and from 1997 to 2000, he was with Beijing Institute of Control Engineering and in charge of satellite control system design. From 1995 to 1997 and since 2000, he has been with China Academy of Space Technology. His research has included guidance, navigation and control of spacecraft. He has been selected a member of International Academy of Astronautics.